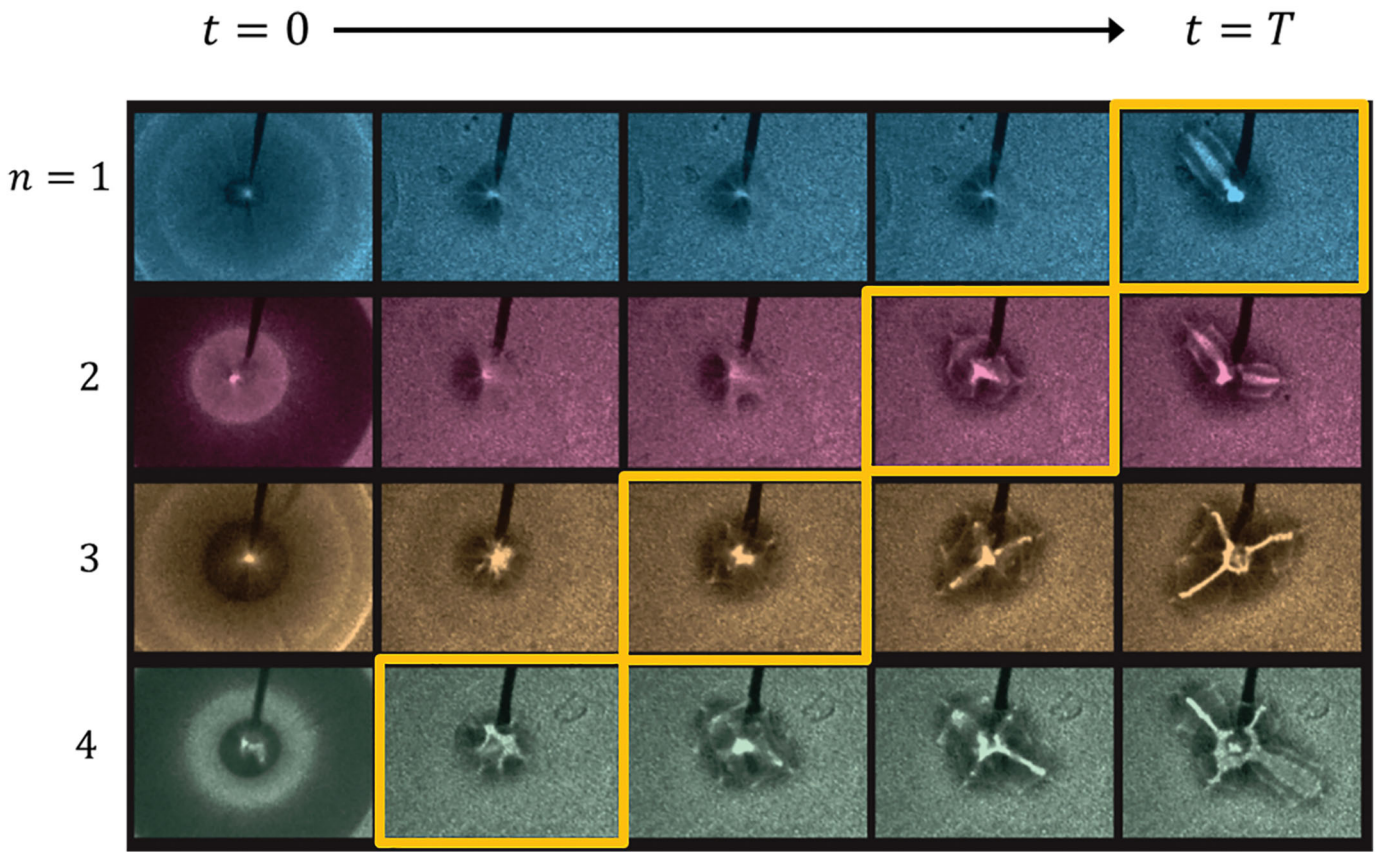

Highlighting experiments performed at North Carolina State University in the lab of Karen Daniels, in collaboration with researchers from Ecole Normale Supérieure de Cachan and Clemson University.

Capillary fracture of ultrasoft gels: variability and delayed nucleation

A surfactant-laden droplet placed on the surface of an ultrasoft gel at time $t = 0$ will produce capillary fractures with n arms after a delay ($t = T$); the histograms of this delay time indicate that the failure is a thermally-activated process.

As featured in:

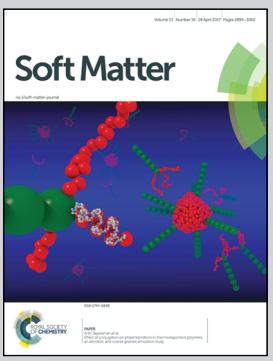

See Karen E. Daniels *et al.*, *Soft Matter*, 2017, **13**, 2962.

ROYAL SOCIETY OF CHEMISTRY

rsc.li/soft-matter-journal

Registered charity number: 207890

Soft Matter

PAPER

Cite this: *Soft Matter*, 2017, 13, 2962

Capillary fracture of ultrasoft gels: variability and delayed nucleation†

Marion Grzelka,[ab] Joshua B. Bostwick[c] and Karen E. Daniels*[b]

Received 6th February 2017,
Accepted 14th March 2017

DOI: 10.1039/c7sm00257b

rsc.li/soft-matter-journal

A droplet of surfactant spreading on an ultrasoft ($E \lesssim 100$ Pa) gel substrate will produce capillary fractures at the gel surface; these fractures originate at the contact-line and propagate outwards in a starburst pattern. There is an inherent variability in both the number of fractures formed and the time delay before fractures form. In the regime where single fractures form, we observe a Weibull-like distribution of delay times, consistent with a thermally-activated process. The shape parameter is close to 1 for softer gels (a Poisson process), and larger for stiffer gels (indicative of aging). For single fractures, the characteristic delay time is primarily set by the elastocapillary length of the system, calculated from the differential in surface tension between the droplet and the substrate, rather than the elastic modulus as for stiffer systems. For multiple fractures, all fractures appear simultaneously and long delay times are suppressed. The experimental protocol provides a new technique for probing the energy landscape and fracture toughness of ultrasoft materials through measurement of the delay time distribution.

1 Introduction

The failure of soft materials is highly relevant to many biological and medical processes such as cellular dynamics[1,2] or drug delivery over mucus membranes.[3,4] These highly-deformable materials, which include gels, elastomers, and biological tissues, can have elastic moduli as low as 10–100 Pa, and are sufficiently soft that they cannot support their own weight when freestanding. Material strength comes from cross-linked polymers that are known to have heterogeneous mechanical properties,[5,6] which makes performing traditional materials tests challenging. In this paper, we present a novel method for probing the strength of ultrasoft materials on the millimeter scale by using the surface tension (capillarity) of liquid droplets to provide well-controlled, but weak, surface forces. Traditional materials tests are not feasible for ultrasoft gels. Our technique draws on both prior experiments on delayed fracture[7] and recent advances in understanding the spreading, wetting, and material failure in this elastocapillary regime.[8–11]

In our experiments, we deposit a droplet of surfactant–water solution on the surface of an agar substrate and observe the formation of starburst-shaped capillary fractures that propagate radially outward from the contact-line. It has previously been observed that the mean number of fractures formed is controlled by the ratio of the surface tension contrast between the droplet σ_d and the gel σ_g, $\Delta\sigma = \sigma_g - \sigma_d$, and the elastic modulus E of the gel substrate.[12] Similar instabilities have been observed on various gel/fluid combinations.[13–15] The focus of this paper is the statistical variability of the fracture process and its relationship to the material properties of ultrasoft substrates. In contrast to typical fracture experiments, which use increasing stress to find a fracture threshold or cyclic load to determine fatigue, we apply a constant force in a technique similar to that of Bonn *et al.*,[7] where agarose gel rods ($E \approx 50$ kPa) were bent to a fixed strain and held until material failure arose through a thermally-activated process. This method allows for probing the energetics of the crosslinks from the statistical distribution of the delay times. We measure histograms for the delay time and number of fractures, revealing that the nucleation process is thermally-activated; this method allows for estimating the typical size of energy barriers.[39]

It is helpful to contrast our approach with classic droplet-spreading experiments on solid,[16] strong gel[17–20] (E = 75–150 kPa) or liquid[21] substrates. The elastocapillary length $\lambda = \sigma_d/E$ sets the scale of elastic deformation in problems involving the interactions between liquids and compliant substrates. For reference, a droplet of water (σ_d = 72 mN m^{-1}) wetting a glass substrate (E = 70 GPa) produces negligible deformations $\lambda \sim 10^{-12}$ m. Recently, attention has shifted to soft substrates.[8,22–31] For example, Jerison *et al.*[8] used fluorescence confocal microscopy to quantify the $\lambda \sim 10^{-6}$ m size deformations produced by a droplet of water on a silicone gel substrate ($E \sim 10$ kPa). The ultrasoft substrates we use in our experiments have an elastic modulus $E \lesssim 100$ Pa with

[a] *Ecole Normale Supérieure de Cachan, 94235 Cachan, France*
[b] *Department of Physics, North Carolina State University, Raleigh, NC, USA. E-mail: kdaniel@ncsu.edu*
[c] *Department of Mechanical Engineering, Clemson University, Clemson, SC, USA*

† Electronic supplementary information (ESI) available. See DOI: 10.1039/c7sm00257b

deformations $\lambda \sim 10^{-3}$ m, large enough to cause the fracture of the substrate. Understanding the various regimes in which elastocapillary deformations are significant will aid in understanding the physics of fracture for soft materials.

2 Experiment

We investigate the fracture of ultrasoft gel substrates, composed of agar (polysaccharide with galactose subunits, Source: BD Difco granulated agar, molecular weight ~1500 daltons[32]) dissolved in deionized water. The concentrations investigated range from ϕ = 0.115–0.127 w% agar, which is above the gel transition at ϕ_c = 0.013% at 20.0 °C.[33] These concentrations correspond to an elastic modulus E = 40–60 Pa.[33] Due to the strong dependence $E(\phi)$ and the aging of gels,[34,35] we find that repeatability of experiments requires careful control of the preparation process. Gels are prepared by dissolving agar powder into 25 mL of deionized water at a temperature of 90 °C. The solution is poured into individual Petri dishes (diameter 9.5 cm) and cooled overnight at room temperature 20.5 ± 0.5 °C. The final thickness of each substrate was measured to be h = 3.0 ± 0.2 mm.

When a liquid droplet is placed on the surface of the gel, surface forces cause fractures to form, as shown in Fig. 1. To control the magnitude of these forces, we utilize Triton X-305 surfactant (Dow Chemical, octylphenoxy polyethoxy ethanol) dissolved in deionized water at concentration χ ranging from 80–300 ppm. The droplet surface tension σ_d varies from 61.2–57 mN m^{-1} with larger χ yielding smaller σ_d.[36] A volume-controlled syringe pump releases droplets of volume V = 21 ± 0.1 μL from a height H = 3.2 cm directly above the center of the gel substrate. For simplicity, we assume the surface tension of the gel σ_g is constant and we observe that the wetting behavior is primarily controlled by the surface tension contrast $\Delta\sigma \equiv \sigma_g - \sigma_d$. Note that the shape of the droplet is also an important factor.[10]

Fractures are visualized using shadowgraphy: a point source of light passes through a converging lens resulting in parallel light that is transmitted through the sample, which is subject to refraction due to the variations in the index of refraction for the gel and the droplet. The image is captured on a ground glass screen located above the sample using a digital camera operating at frequency f = 15 Hz. Our technique allows for the measurement of both the number of fractures n and the delay time T before fractures initiate. We calculate both the time t = 0 when the droplet first contacts the substrate, and the delay time T when a fracture forms, *via* an *ad hoc* image-processing code that identifies changes in the standard deviation of the image light intensity.

Table 1 Experimental parameters for the four data series, with $\Delta\sigma$ calculated for σ_g = 69 mN m^{-1} for all gels. Errors in material parameters are E: ±1.5 Pa, σ_d: ±0.1 mN m^{-1}

Series	ϕ [%]	E [Pa]	χ [ppm]	σ_d [mN m^{-1}]	$\delta = \frac{\Delta\sigma}{E}$ [mm]	$\lambda = \frac{\sigma_d}{E}$ [mm]
1	0.115	41.1	80	61.2	0.19	1.49
2	0.115	41.1	200	59.0	0.24	1.44
3	0.123	52.5	250	58.0	0.21	1.10
4	0.127	59.1	300	57.0	0.20	0.96

In previous work, Daniels *et al.*[12] observed significant variation in the number of fractures observed for a fixed set of experimental parameters (σ_d,E). In order to probe how such variation arises, as well as the statistics of thermal activation, we minimize this variability. In addition to the strategies mentioned above (aging gels for a consistent time and using a syringe pump to deposit droplets), we embed the entire apparatus in a sandbox to damp out the acoustic noise and building vibrations that can prematurely initiate fractures. Variations in the degree of surface contamination are present as well, and were minimized by cooling the gels in a covered environment. To obtain statistics to quantify these variations, we perform experiments on approximately 1200 samples divided among the four series listed in Table 1. This range of values produces starbursts with n = 0 to n = 4 fractures.

3 Results

It has been previously reported[12] that the mean number of fractures $\langle n \rangle$ increases as a function of the quantity $\delta \equiv \Delta\sigma/E$ related to the elastocapillary length λ; note that δ and λ have the opposite trend with σ_d. We quantify our results using both δ and λ assuming σ_g = 69 mN m^{-1} for agar.

As illustrated in Fig. 1, fractures do not necessarily nucleate immediately after the droplet is placed on the gel substrate, but after some delay T. Here, the elastic deformations induced by the wetting forces between the droplet and the gel[8,10,24,37] produce a state of stress that is not quite large enough to cause material failure. The gel remains in this deformed elastic state until failure occurs by external perturbation or a thermal fluctuation.

To quantify the dependence of the delay time T on the properties of the gel substrate, we select three pairs of (E,σ_d) values for which n = 1 is highly likely (Fig. 2). (This was done

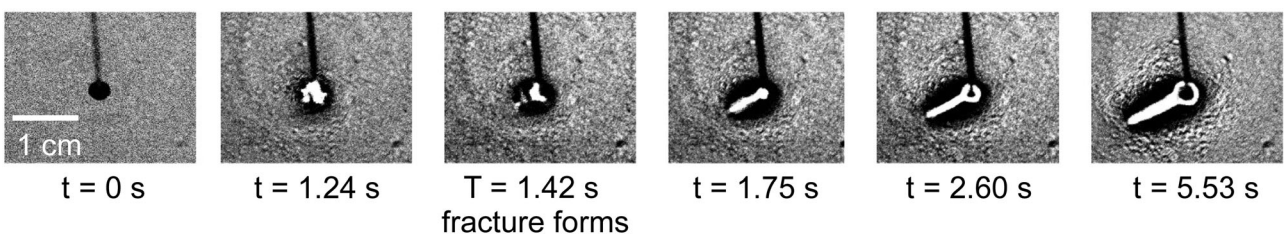

Fig. 1 Typical delayed fracture time evolution from Series 1 (Table 1); a needle deposits a droplet at t = 0 s and a fracture with n = 1 is nucleated at t = 1.42 s that propagates outwards from the contact-line.

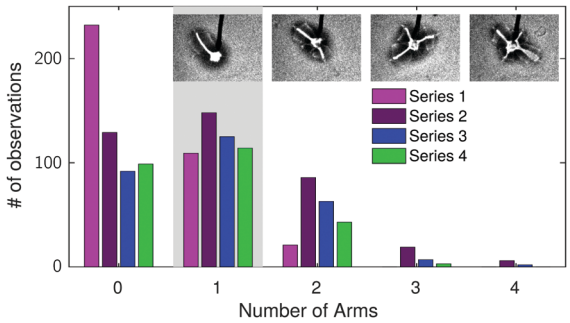

Fig. 2 Histogram of the number of fractures n formed for each of the data series given in Table 1. The set of runs with $n = 1$ (gray rectangle) form the basis of our analyses. Series 2 is used to investigate multiarm statistics, and sample images are drawn from this series.

empirically by selecting three values of E, and varying σ_d (equivalently $\Delta\sigma$) until we observed $n = 1$ fractures in approximately 1/3 of the trials.) These pairs correspond to approximately constant $\delta \approx 0.2$ mm, a length consistent with the size of observed surface deformations.[12] One set of parameters (Series 1) provides a control series by matching the value of E for Series 2 for different $\Delta\sigma$, while still maintaining $n = 1$ as a highly likely outcome. Series 3 and 4 necessarily increase E and decrease σ_d in order to maintain an approximately consistent histogram $\mathscr{P}(n)$. Maintaining this consistent $\mathscr{P}(n)$ significantly restricts the range of parameters we explore. An additional advantage of Series 2 is that it provides enough data for $n > 1$ that we can perform a semi-quantitative investigation of the delay statistics of multiarm $n > 1$ starbursts.

We begin by analyzing the set of starbursts with $n = 1$. For all four series, we observe delay times as long as a minute. Fig. 3 shows the survival function (complementary cumulative distribution) or probability that a droplet survives less than time T before producing fracture(s). Using Matlab's wblfit( ) tool, we fit each waiting time distribution to a Weibull distribution:

$$\mathscr{P}(T) = \left(\frac{\beta}{\tau}\right)\left(\frac{T}{\tau}\right)^{\beta-1} e^{-(T/\tau)^{\beta}} \quad (1)$$

as shown in Fig. 3. The corresponding form for the survival function is a stretched exponential $S(T) = e^{-(T/\tau)^{\beta}}$, which appears as a straight line when plotting log(S) on log–log axes (see Fig. 3 inset). The Weibull plot (inset) reveals all datasets to be highly linear for large T. Inevitably, the low-T portion of the histogram contains an excess of data, triggered by non-thermal noise. For example, when we collect data in the presence of additional room noise, we observe that the delay times are systematically reduced from the observations shown here.

The fit parameters (τ,β) carry two important interpretations to aid in understanding delayed fracture. The parameter τ represents a characteristic delay time and the parameter β a shape parameter. For the special case $\beta = 1$, the Weibull distribution reduces to an exponential distribution, corresponding to Poisson-distributed events with constant failure rate. For this case (only), τ is identical to the mean delay time $\langle T \rangle$. The shape parameter β is necessary to fit the non-monotonic histograms (*cf.* Fig. 3a); $\beta > 1$ indicates that the system ages such that failure is more likely the longer the delay.

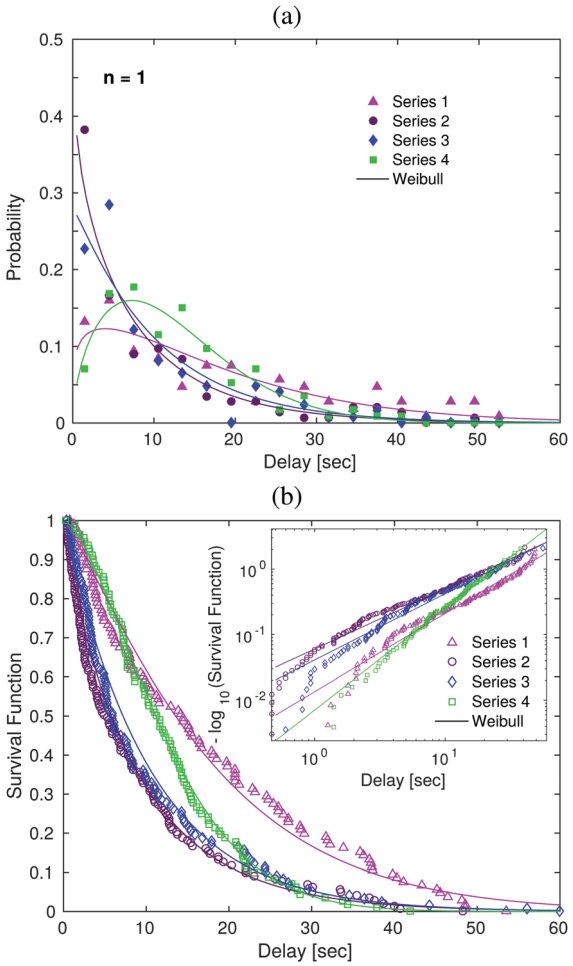

Fig. 3 (a) Histograms and (b) survival function of measured delay times T for the experimental parameters given in Table 1, on the subset of data with $n = 1$ arms. Solid curves are numerical fits to a Weibull distribution.

Fig. 4 examines how the material parameters set the failure dynamics through β and τ. For Series 2 & 3, $\beta \approx 1$ and $\tau \approx \langle T \rangle$ consistent with a thermally-activated Poisson process.[7] We observe $\beta > 1$ in the two cases (Series 1 & 4) with non-monotonic histograms (*cf.* Fig. 3a), which indicates these gels age in a way that weakens them as a function of time elapsed since loading. Interestingly, Series 1 & 4 have the least in common when examined in light of their materials parameters (Table 1). We observe that β increases with E (Fig. 4b), but does not monotonically depend on any of the other materials parameters.

The characteristic delay time τ is observed to decrease with increasing δ (*cf.* Fig. 4h), implying that larger deformations δ lead to shorter delays before fracture. The decreasing trend is robust when considering other reasonable values of the gel surface tension $65 < \sigma_g < 71$ mN m^{-1} (see Appendix). Over this same range of σ_g values, no systematic trend is observed for the traditional elastocapillary length λ,[8,9] suggesting the surface tension differential $\Delta\sigma$ instead determines the size of the characteristic force in our experiment.

For starbursts with multiple arms, we observe that all of the fractures occur simultaneously, and that delay times are shorter

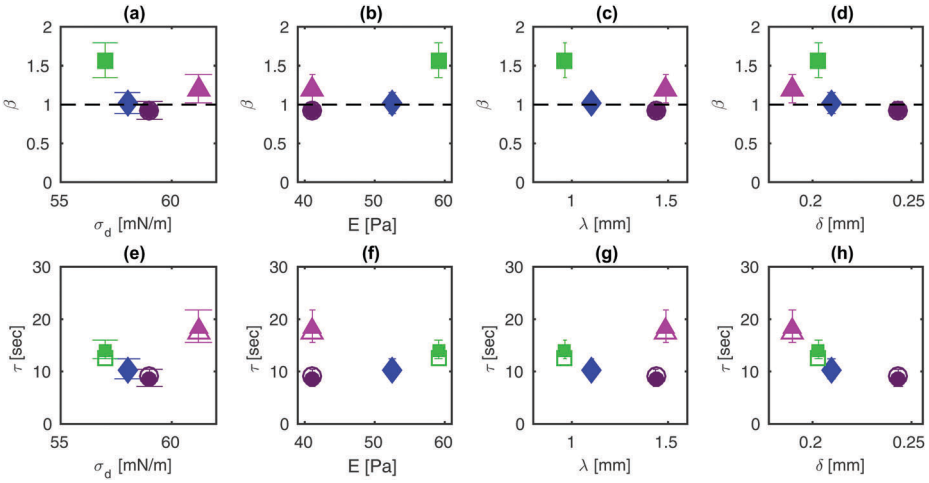

Fig. 4 Weibull parameters as a function of materials parameters for $n = 1$ from the four data series. (a–d) Shape parameter β and (e–h) Weibull delay time τ (solid symbols) with mean delay time $\langle T \rangle$ (open symbols). Error bars are 95% confidence intervals on the fit parameters. See ESI† for alternative versions with varying values of σ_g.

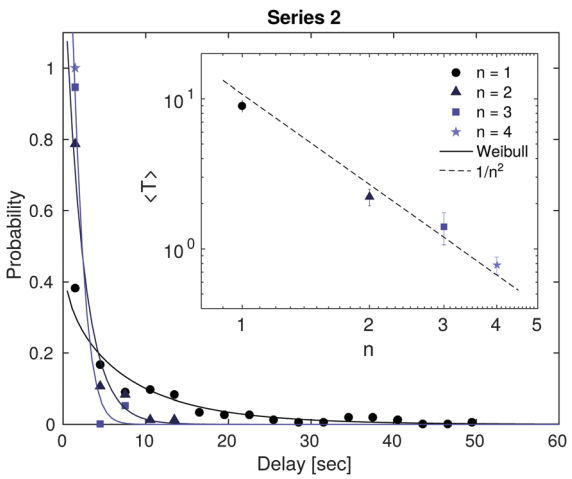

Fig. 5 Histogram of measured delay times T for starbursts with a variable number of arms, all from Series 2. (inset) Mean delay time $\langle T \rangle$ as a function of the number of arms (error bars are standard error).

than for the $n = 1$ case analyzed above. This suggests that once one fracture is initiated by a thermal fluctuation, it triggers the simultaneous nucleation of the other fractures. Using the data from Series 2, for which up to $n = 4$ fractures were observed, we have sufficient statistics to perform a semi-quantitative investigation. As shown in Fig. 5, we observe that delay times are reduced by a factor proportional to $1/n^2$ for starbursts with multiple arms. For $1 \leq n \leq 3$, the dynamics are consistent with a Poisson process ($\beta = 1$ within error bars); for $n = 4$ there is insufficient data.

4 Discussion

A liquid droplet deforms an ultrasoft agar substrate to the point of material failure, resulting in the nucleation of fractures at the contact line which propagate radially outward in a starburst formation. The mean number of fractures $\langle n \rangle$ is controlled by the ratio of the surface tension contrast $\Delta\sigma$ to the elastic modulus E of the gel substrate.[12] We quantify the statistical variations in both the delay time before fractures form, and the number of fractures within the starburst. While the experiments reported here utilize a single pair of materials (agar, Triton X-305), the same phenomenon also occurs for other gel and droplet materials.[12–14] In particular, we previously observed[12] that similar delays are observed when the droplet and substrate are immiscible (agar, PDMS oil) and diffusive effects are negligible. Future studies should be undertaken to probe the specific effects of diffusion, miscibility, salt concentration, gel viscoelasticity, and other gel/droplet parameters.

For a given set of experimental parameters (fixed E, σ_d, V), the number of fractures within each starburst has a well-defined mean, but is not deterministic. Instead, there is a range of observed values whose variability likely arises from both the inherent heterogeneity of the gels[5] and the presence of multiple unstable deformation modes.[10] The significant heterogeneity we observe at small E is consistent with models of critical fluctuations on approach to the gel transition.[5]

By isolating the case of single-arm starbursts ($n = 1$), we infer from the exponential (or Weibull) distribution of delay times that the fracture process is thermally-activated. This effect has previously been observed in systems which are 1000 times stiffer and subject to different loading conditions,[7] highlighting the universality of delayed fracture dynamics. Our novel experimental protocol can then probe the properties of ultrasoft materials that are not suited for standard failure tests.

For a purely thermally-activated process, the delay time distribution $\mathscr{P}(T)$ would be exponential with $\tau = \langle T \rangle$ set by the height of the energy barriers in the material. We note that the mean delay time $\langle T \rangle$ is inversely proportional to the thermal nucleation probability $\mathscr{P} \propto \exp(-\mathscr{E}_{act}/k\mathscr{T})$, and is thereby a measure of the activation energy $\mathscr{E}_{act}$.[7,39] Because τ (or $\langle T \rangle$) is not a constant function of agar concentration χ (or modulus E), our results suggest the energy associated with the crosslinking

of agar is not the only effect. Instead, we observe a trend in which the length scale $\delta = \Delta\sigma/E$ controls the timescale τ. We interpret this finding as highlighting the importance of the differential in surface tension between the droplet and the gel substrate, despite λ traditionally appears in elastocapillary phenomena such as wrinkling, blistering, and stiction.[38] Intriguingly, it appears that E is additionally important in controlling the shape parameter β of the Weibull distribution, not just the energy barriers, due to its effects on gel aging.[34,35] Future experiments could use this technique to map out, and disentangle, the effects of aging on the energy barrier landscape in soft materials.

Acknowledgements

We would like to thank Michael Shearer and Carlos Ortiz for useful discussions, and Mark Schillaci for crucial upgrades to the experimental protocol. We are grateful for support from the National Science Foundation under grant number DMS-0968258.

References

1 I. Levental, P. Georges and P. Janmey, *Soft Matter*, 2007, **3**, 299.
2 G. Beaune, T. V. Stirbat, N. Khalifat, O. Cochet-Escartin, S. Garcia, V. V. Gurchenkov, M. P. Murrell, S. Dufour, D. Cuvelier and F. Brochard-Wyart, *Proc. Natl. Acad. Sci. U. S. A.*, 2014, **111**, 8055.
3 K. Khanvilkar, M. D. Donovan and D. R. Flanagan, *Adv. Drug Delivery Rev.*, 2001, **48**, 173.
4 J. J. Haitsma, U. Lachmann and B. Lachmann, *Adv. Drug Delivery Rev.*, 2001, **47**, 197.
5 P. Goldbart and N. Goldenfeld, *Phys. Rev. A: At., Mol., Opt. Phys.*, 1989, **39**, 1402.
6 M. A. Meyers, P.-Y. Chen, A. Y.-M. Lin and Y. Seki, *Prog. Mater. Sci.*, 2008, **53**, 1.
7 D. Bonn, H. Kellay, M. Prochnow, K. Ben-Djemiaa and J. Meunier, *Science*, 1998, **280**, 265.
8 E. Jerison, Y. Xu, L. Wilen and E. Dufresne, *Phys. Rev. Lett.*, 2011, **106**, 186103.
9 S. Das, A. Marchand, B. Andreotti and J. H. Snoeijer, *Phys. Fluids*, 2011, **23**, 072006.
10 J. B. Bostwick and K. E. Daniels, *Phys. Rev. E: Stat., Nonlinear, Soft Matter Phys.*, 2013, **88**, 042410.
11 J. B. Bostwick, M. Shearer and K. E. Daniels, *Soft Matter*, 2014, **10**, 7361.
12 K. E. Daniels, S. Mukhopadhyay, P. Houseworth and R. P. Behringer, *Phys. Rev. Lett.*, 2007, **99**, 124501.
13 C. Spandagos, T. B. Goudoulas, P. F. Luckham and O. K. Matar, *Langmuir*, 2012, **28**, 7197.
14 C. Spandagos, T. B. Goudoulas, P. F. Luckham and O. K. Matar, *Langmuir*, 2012, **28**, 8017.
15 G. Foyart, L. Ramos, S. Mora and C. Ligoure, *Soft Matter*, 2013, **9**, 7775.
16 L. Tanner, *J. Phys. D: Appl. Phys.*, 1979, **12**, 1473.
17 D. Szabo, S. Akiyoshi, T. Matsunaga, J. P. Gong, Y. Osada and M. Zrinyi, *J. Chem. Phys.*, 2000, **113**, 8253.
18 D. Kaneko, J. P. Gong, M. Zrinyl and Y. Osada, *J. Polym. Sci., Part B: Polym. Phys.*, 2005, **43**, 562.
19 M. Banaha, A. Daerr and L. Limat, *Eur. Phys. J.: Spec. Top.*, 2009, **166**, 185.
20 T. Kajiya, A. Daerr, T. Narita, L. Royon, F. Lequeux and L. Limat, *Soft Matter*, 2013, **9**, 454.
21 D. P. Hoult, *Annu. Rev. Fluid Mech.*, 1972, **4**, 341.
22 R. Pericet-Cámara, A. Best, H. J. Butt and E. Bonaccurso, *Langmuir*, 2008, **24**, 10565.
23 T. Kajiya, A. Daerr, T. Narita, L. Royon, F. Lequeux and L. Limat, *Soft Matter*, 2011, **7**, 11425.
24 S. Das, A. Marchand, B. Andreotti and J. H. Snoeijer, *Phys. Fluids*, 2011, **23**, 072006.
25 R. W. Style and E. R. Dufresne, *Soft Matter*, 2012, **8**, 3177.
26 A. Marchand, S. Das, J. H. Snoeijer and B. Andreotti, *Phys. Rev. Lett.*, 2012, **108**, 094301.
27 J. H. Weijs, B. Andreotti and J. H. Snoeijer, *Soft Matter*, 2013, **9**, 8494.
28 D. L. Henann and K. Bertoldi, *Soft Matter*, 2014, **10**, 709.
29 S. J. Park, B. M. Weon, J. J. S. Lee, J. J. S. Lee, J. Kim and J. H. Je, *Nat. Commun.*, 2014, **5**, 4369.
30 R. W. Style, A. Jagota, C.-Y. Hui and E. R. Dufresne, *Annu. Rev. Condens. Matter Phys.*, 2017, **8**, DOI: 10.1146/annurev-conmatphys-031016-025326.
31 B. Andreotti and J. H. Snoeijer, *EPL*, 2016, **113**, 66001.
32 F. Marga, L. Vebret and H. Morvan, *Plant Cell, Tissue Organ Cult.*, 1997, **49**, 1.
33 M. Tokita and K. Hikichi, *Phys. Rev. A: At., Mol., Opt. Phys.*, 1987, **35**, 4329.
34 G. W. Scherer, *J. Non-Cryst. Solids*, 1988, **100**, 77.
35 I. M. Hodge, *Science*, 1995, **267**, 1945.
36 J. Zhang, C. Daubert and E. Foegeding, *J. Food Sci.*, 2005, **70**, e425.
37 A. Bardall, K. E. Daniels and M. Shearer, http://arxiv.org/abs/1607.01637.
38 B. Roman and J. Bico, *J. Phys.: Condens. Matter*, 2010, **22**, 493101.
39 Y. Pomeau, *C. R. Acad. Sci., Ser. II: Mec., Phys., Chim., Sci. Terre Univers*, 1992, **314**, 553.

